

LETTER • OPEN ACCESS

Rising methane emissions from boreal lakes due to increasing ice-free days

To cite this article: Mingyang Guo *et al* 2020 *Environ. Res. Lett.* **15** 064008

View the [article online](#) for updates and enhancements.

Recent citations

- [Patterns and isotopic composition of greenhouse gases under ice in lakes of interior Alaska](#)
Madeline O'Dwyer *et al*

Environmental Research Letters



LETTER

Rising methane emissions from boreal lakes due to increasing ice-free days

OPEN ACCESS

RECEIVED
21 January 2020

REVISED
5 March 2020

ACCEPTED FOR PUBLICATION
23 March 2020

PUBLISHED
19 May 2020

Original content from this work may be used under the terms of the [Creative Commons Attribution 4.0 licence](#).

Any further distribution of this work must maintain attribution to the author(s) and the title of the work, journal citation and DOI.



Mingyang Guo¹, Qianlai Zhuang^{1,2}, Zeli Tan³, Narasinha Shurpali⁴, Sari Juutinen⁵, Pirkko Kortelainen⁶ and Pertti J Martikainen⁴

¹ Purdue University, West Lafayette, IN, United States of America

² Purdue Climate Change Research Center, West Lafayette, IN, United States of America

³ Pacific Northwest National Laboratory, Richland, WA, United States of America

⁴ University of Eastern Finland, Kuopio, Finland

⁵ University of Helsinki, Helsinki, Finland

⁶ Finnish Environment Institute, Helsinki, Finland

E-mail: qzhuang@purdue.edu

Keywords: methane emission, boreal lake, climate change

Supplementary material for this article is available [online](#)

Abstract

Lakes account for about 10% of the boreal landscape and are responsible for approximately 30% of biogenic methane emissions that have been found to increase under changing climate. However, the quantification of this climate-sensitive methane source is fraught with large uncertainty under warming climate conditions. Only a few studies have addressed the mechanism of climate impact on the increase of northern lake methane emissions. This study uses a large observational dataset of lake methane concentrations in Finland to constrain methane emissions with an extant process-based lake biogeochemical model. We found that the total current diffusive emission from Finnish lakes is 0.12 ± 0.03 Tg CH₄ yr⁻¹ and will increase by 26%–59% by the end of this century depending on different warming scenarios. We discover that while warming lake water and sediment temperature plays an important role, the climate impact on ice-on periods is a key indicator of future emissions. We conclude that these boreal lakes remain a significant methane source under the warming climate within this century.

1. Introduction

Atmospheric methane (CH₄) is the second major greenhouse gas after carbon dioxide. Although it only contributes to about 20% of the warming effect, its global warming potential is 28 times higher than carbon dioxide (Lashof *et al* 1990, Myhre *et al* 2013, IPCC 2014). Over the past two decades, surface freshwater including lakes, reservoirs, streams and rivers has been receiving an accumulating attention as important global methane sources (Bastviken *et al* 2011, Prairie *et al* 2013, Saunio *et al* 2016). However, studies have shown large uncertainties in the estimation of freshwater methane emissions (Kirschke *et al* 2013). A better estimation of the present and future lake methane emissions would largely benefit from critical improvement in watercourse mapping and methane flux measurements (Saarnio *et al* 2009; Kirschke *et al* 2013). Furthermore, previous studies mostly focused on quantitative estimation but hardly

explored the mechanisms of how climate warming indeed affects lake methane emissions.

Finland has one of the densest inland water systems in the world with over 200 000 (Raatikainen and Kuusisto 1990) freshwater bodies covering an area greater than 33 000 km² over the whole country. Nearly all the lakes are in the boreal region. Ranta10 (Finnish Environment Institute 2016) is a topologically corrected spatial dataset. It contains geographical coordinate and area information of 214 995 lakes, covering 37 595 km² of the land surface. It is higher in spatial resolution than the more commonly used Global Lakes and Wetlands Database (GLWD) which only comprises 2202 lakes and reservoirs covering around 20 194 km² in Finland. The Ranta10 database offers a unique opportunity for modeling exercises since the smaller lakes are found to have higher methane fluxes per unit area (Juutinen *et al* 2009, Holgerson *et al* 2016, Sasaki *et al* 2016) and are more sensitive to climate change (Sanchez *et*

al 2019). Additionally, (Juutinen *et al* (2009) have provided the measured water temperature, nutrients and methane concentrations for the studies 207 Finnish lakes.

By using these datasets, we can not only evaluate methane emissions from the boreal lakes in Finland under climate change through modeling but also further explore the driving factors of emissions from a mechanistic perspective, which shall help future prediction of the emissions under climate change. Also, we extrapolate our model to the whole Arctic freshwater system for both historical and future periods.

2. Materials and methods

2.1. Model configuration

The Arctic Lake Biogeochemistry Model (ALBM) is a one-dimensional process-based lake biogeochemical model designed for predicting both thermal and carbon dynamics of aquatic ecosystems. It mainly consists of several modules including those for the radiative transfer, the water/sediment thermal circulation, the water/sediment biogeochemistry, and the gas diffusive and ebullition transportation. Although this model was originally developed for Arctic lakes (Tan *et al* 2015a), it can achieve comparable or even better performance than those widely used one-dimensional lake models in representing the physical and biogeochemical processes of other northern lakes (Guseva *et al* 2020). Detailed information about ALBM can be found in Tan *et al* (2015a, 2017, 2018). We introduce the key governing equations of methane processes in ALBM below.

Methane production rate P ($\mu\text{mol m}^{-3} \text{s}^{-1}$) in sediments is calculated from labile carbon content and temperature:

$$P = R_c C_{\text{labile}} P Q_{10}^{(T-T_{pr})/10} \quad (1)$$

where R_c is the fraction of carbon decomposed per second (s^{-1}), C_{labile} is the labile carbon content ($\mu\text{mol m}^{-3}$), PQ_{10} is the factor by which the production rate increases with a 10°C rise in temperature, and T_{pr} is a reference temperature ($^\circ\text{C}$). Methane can be oxidized after released into the water and the oxidation rate V_{oxid} ($\mu\text{mol m}^{-3} \text{s}^{-1}$) is described by

$$V_{\text{oxid}} = Q_{CH_4} OQ_{10}^{(T-T_{or})/10} \frac{C_{O_2}}{k_{O_2} + C_{O_2}} \frac{C_{CH_4}}{k_{CH_4} + C_{CH_4}} \quad (2)$$

where Q_{CH_4} is the maximum oxidation potential ($\mu\text{mol m}^{-3} \text{s}^{-1}$), OQ_{10} is the factor by which the oxidation potential increases with a 10°C rise in temperature, T_{or} is a reference temperature ($^\circ\text{C}$), C_{O_2} and C_{CH_4} are gas concentrations ($\mu\text{mol m}^{-3}$), and k_{O_2} and k_{CH_4} are the Michaelis-Menten constants

($\mu\text{mol m}^{-3}$). Together, the modeled methane concentration in water columns is calculated by

$$\frac{\partial C_{CH_4}}{\partial t} = \frac{\partial}{\partial z} \left(D_{CH_4} \frac{\partial C_{CH_4}}{\partial z} \right) - V_{\text{oxid}} \pm L_{CH_4} \quad (3)$$

where D_{CH_4} is the diffusivity of methane ($\text{m}^2 \text{s}^{-1}$), and L_{CH_4} is the gas exchange between bubbles and the ambient water ($\mu\text{mol m}^{-3} \text{s}^{-1}$). Finally, methane within water is transported to the atmosphere. The diffusive transfer velocity k (m s^{-1}) is defined as

$$k = \sqrt{(0.00015U)^2 + \left(0.07(-\beta Z_{AML})^{\frac{1}{3}}\right)^2} \times Sc_m^{-0.5} \quad (4)$$

where U is the wind speed at 2 m (m s^{-1}), β is buoyant flux ($\beta < 0$ if losing heat and vice versa), Z_{AML} is the depth of the actively mixing layer (m), and Sc_m is the Schmidt number of methane. Since we lacked ebullition flux observations and therefore, we were unable to validate the modeled ebullition emissions, we only quantified diffusive emissions in this study.

The numerical experiment consists of three steps: (1) the model calibration using observations of diffusive emissions during 1998–1999 from 39 individual lakes; (2) regional simulations of 1990–1999 by applying ALBM to the Ranta10 data product; (3) regional simulations of 2010–2019 and 2090–2099 under the representative concentration pathway (RCP) scenarios of RCP4.5 and RCP8.5. For all the simulations, a spin-up period of two years was run.

2.2. Data

Model forcing data include air temperature, surface pressure, 10 m wind, relative humidity, precipitation, snowfall, downward short-wave radiation and downward long-wave radiation. The historical simulation was driven by the climate data retrieved from the European Center for Medium-Range Weather Forecasts (ECMWF) Interim re-analysis (ERA-Interim, Dee *et al* 2011) with a resolution of $0.75^\circ \times 0.75^\circ$, and organized into daily datasets. For future climate scenarios, we used a down-scaled bias-corrected dataset of the Intersectoral Impact Model Intercomparison Project (ISIMIP) output from HadGEM2-ES (Frieler *et al* 2017) that is set on a $0.5^\circ \times 0.5^\circ$ global grid and is divided into daily time steps. This climate dataset is bias-corrected based on ERA-Interim, which guarantees the consistency of historical and future simulation results.

Lakes with an area smaller than 200 m^2 were omitted in our simulations due to the large uncertainties in the mapping of these lakes, leaving 176 876 lakes covering $36 690 \text{ km}^2$. In general, the region north of 67°N has the highest lake density but relatively sparse observations of thermal or carbon dynamics (figures 1(a) and 1(b)). Over 90% of the lakes are smaller than 0.1 km^2 (figure 1(c)), which are not included in the GLWD-3 database. Depth information was lacking for over 90% of the lakes even by combining

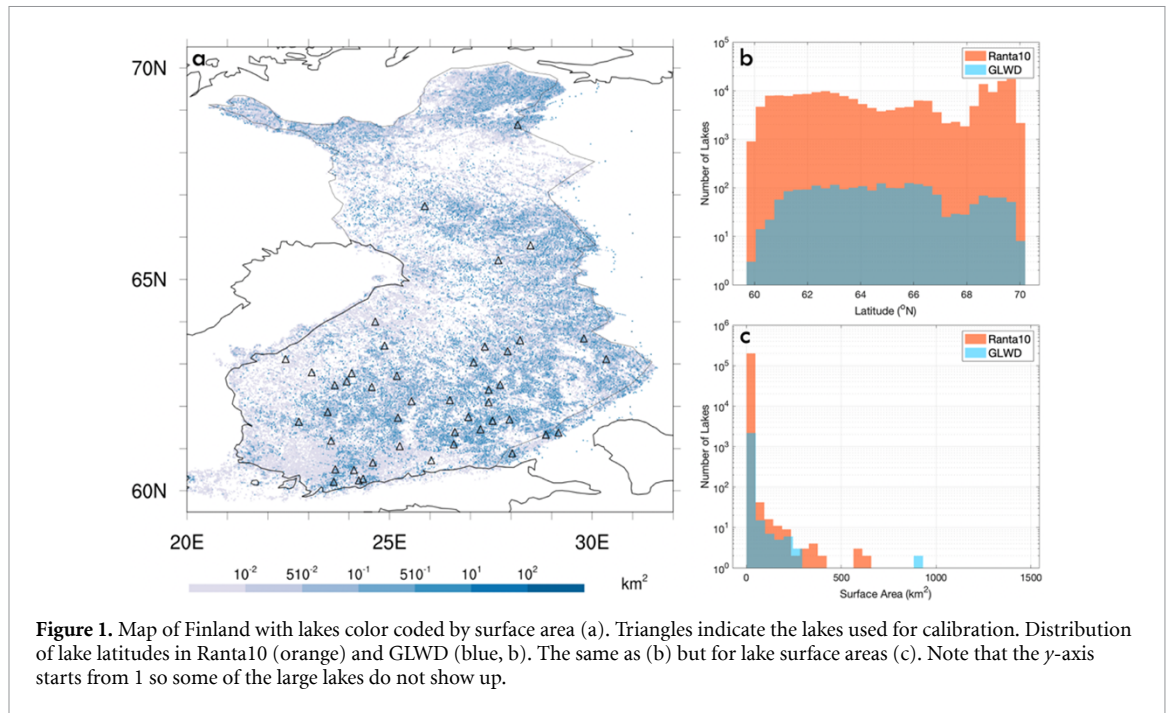


Figure 1. Map of Finland with lakes color coded by surface area (a). Triangles indicate the lakes used for calibration. Distribution of lake latitudes in Ranta10 (orange) and GLWD (blue, b). The same as (b) but for lake surface areas (c). Note that the y-axis starts from 1 so some of the large lakes do not show up.

the Ranta10 and the GLWD-3 database. As such, we applied a statistical approach to construct the full lake depth dataset. We first grouped the lakes into 10 bins bounded by areas of 0, 0.01, 0.05, 0.1, 0.5, 1, 2, 3, 4, 5, 10, 100, 1500 km², respectively. We then generated a histogram of depths in each group. We randomly assigned the depths following the fitted probability distribution in each group. By following this approach, we aimed to construct lakes profiles that match the diversity of the real lake system in Finland. In terms of lake bathymetry, we assume a linear decrease of the cross-section area with increasing depth.

Water temperature, nutrient and methane concentrations were measured at four levels of depth four times (before and after ice melt, late summer and autumn circulation) either in the 1998 or 1999. The diffusive methane fluxes were calculated following equation (4) (see also Juutinen *et al* 2009). For the simulation purpose, several assumptions and approximations were made on for carbon and phosphorous input that is required by the model, including (1) dissolved organic carbon (DOC) concentration is equal to total organic carbon (Mattsson *et al* 2005, Kortelainen *et al* 2006, Mopper *et al* 2006); (2) dissolved inorganic carbon (DIC) concentration is calculated from pH and alkalinity; (3) soluble reactive phosphorus (SRP) concentration is equal to PO₄ and (4) particular organic carbon (POC) concentration is approximately 1/5.1 of DOC concentration (Rachold *et al* 2014). We produced an input map of DOC, DIC, PO₄ and SRP at 1° × 1° with observations averaged at each grid and filled with nearest-neighbor interpolation (figure S1 (stacks.iop.org/ERL/15/064008/mmedia)).

2.3. Model calibration

Since the lake shape has large impacts on the thermal dynamics (Mazumder and Taylor 1994, Woolway *et al* 2016, Woolway and Merchant 2017) and carbon dynamics (Schilder *et al* 2013, Pighini *et al* 2018), we decided to conduct calibration and thus simulations by lake groups. The simulated lakes were firstly divided by the surface area into six groups bounded by 0, 0.05, 0.1, 0.2, 1, 10, 1500 km², respectively and then by the shape factor, defined by $\sqrt{\text{Area}}/\text{Depth}$, into two groups bounded by 0, 0.1 and 10, respectively. Thirty-nine lakes that represent various depths and shape factors were used for calibration.

We calibrated the parameters related to water temperature (Ks, Cps, Pi, Rous, Roun, Feta, Wstr and Ktscale) and methane diffusive emission (OQ10, QCH4, KCH4, PQ10 n, Rcn and Rca as in equations (1) ~ (4)). The detailed descriptions and corresponding ranges of the parameters are listed in table S1. Since the sensitive parameters of the water temperature and the methane diffusive emission simulations were different, the calibration was conducted separately. We first applied a Monte Carlo calibration method for water temperature calibration using 6000 sets of parameters for each lake. For the methane emissions, a ‘history matching’ method (Mcneall *et al* 2013, Williamson *et al* 2013, 2015, 2016) was adopted for higher accuracy and efficiency. This method requires less computation time than a full Monte Carlo simulation (Williamson *et al* 2013) and has been shown to largely reduce simulation biases (Salter *et al* 2019). It was carried out in the following steps: (1) use the Sobol sequence sampling method (Sobol’ 1967) to generate a perturbed parameter ensemble

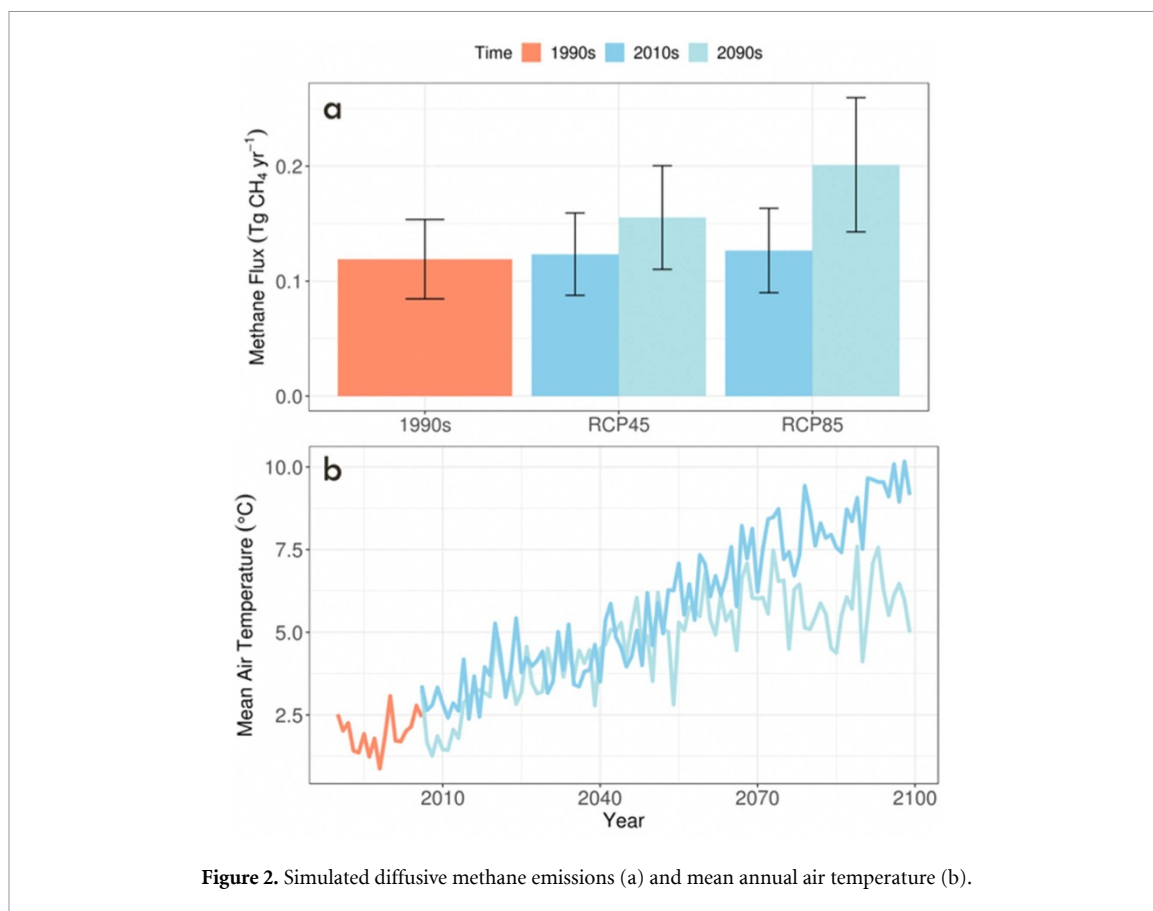


Figure 2. Simulated diffusive methane emissions (a) and mean annual air temperature (b).

(PPE) by sampling from the parameter space; (2) run simulations for all perturbed parameter (PP) sets; (3) rule out regions of the parameter space based on the outputs where a predefined metric exceeds the threshold; (4) repeat step 1–3 until a certain number of iterations or the desired outcome is achieved. In our study, 1200 PP sets were generated for each round and the metric used was the root-mean-square error (RMSE). Parameter spaces resulting in RMSEs over the 50% of the observations at each site were ruled out at each round, until 3 rounds were finished.

2.4. Sensitivity and uncertainty analysis

For parametric sensitivity analysis, running the model for the whole region over a 10-year time period takes about five days, and thus it would be rather time-consuming to run full PPE simulations. Instead, we run short PPE simulations for a single year from 1998 to 1999 with 20 PP sets sampled from the remaining parameter space after history matching. It has been proved that the results from short simulations match well to the longer-term simulations (Yun *et al* 2016), especially when methane emission response to air temperature is a relatively well-defined process (Sanches *et al* 2019) and thus can be captured within a one-year range.

3. Results and discussion

3.1. Model performance

The model overall showed good performances on reproducing both water temperature and methane emissions (table 1) with an average RMSE of 1.59 °C for full-profile water temperature simulations and a correlation coefficient (r) of 0.69 for methane emissions. There was a lake with an estimated methane flux over 200 mmol m⁻² yr⁻¹ while the corresponding modeled value was only one-third of the observed value. This underestimation was possibly due to the missing of DOC concentration measurement at this lake. Since it is a very humic shallow lake (color >90 Pt mg l⁻¹, mean depth <3 m, see Juutinen *et al* 2009), taking the average value of other lakes in the same grid likely results in a much lower DOC concentration. The metrics without considering this lake are also listed in table 1.

Note that the uncertainty range can be wider using the history matching approach than using the Bayesian method, which is expected because the former focuses on confining the output whereas the latter on confining the input, i.e. the parameters themselves. Therefore, the PPE by the latter would be more representative of the parameter distributions and thus results in smaller uncertainties.

Table 1. RMSE and *r* values of water temperature and methane flux simulations. Values in brackets are calculated without considering the very humic shallow lake.

	Annual mean full-profile water temperature	Annual mean methane flux
RMSE	1.59 °C	32.91 (24.07) mmol m ⁻² yr ⁻¹
R	0.94, <i>p</i> < 0.0001	0.69 (0.76), <i>p</i> < 0.0001

3.2. Annual methane emission estimation

Simulations indicated that the methane emissions from Finnish lakes were 0.12 ± 0.03 Tg CH₄ yr⁻¹ in the 1990 s. There was only a 4% and 6% increase during the period 1990 ~ 2019 under RCP4.5 and RCP8.5, respectively (figure 2) when less than 2 °C of warming has occurred. Walter *et al* (2007) estimated that the current total diffusion from all lakes north of 45 °N is 1.12 ± 0.22 Tg CH₄ yr⁻¹. If assuming the same total lake area over the Arctic and the same lake size distribution as the Finnish lakes (Text S1), we estimated the emission to be 3.65 ± 1.06 Tg CH₄ yr⁻¹. The difference can be due to: (1) Walter *et al* (2007) simply used a constant flux calculated from several glacial lakes and thermokarst lakes for all other lakes, which may underrepresent the variation; (2) Based on several Siberian thaw lakes, an ice-free period of 120 d was assumed in the calculation for all lakes, leading to underestimation in warmer regions, for example, the mean ice-off periods in Finland is about 170 d.

We estimate that the Finnish lake diffusive methane emission will increase by 25.8% from 0.12 ± 0.04 to 0.16 ± 0.05 Tg CH₄ yr⁻¹ under the RCP4.5 scenario while it will increase by about 58.9% from 0.13 ± 0.04 to 0.20 ± 0.06 Tg CH₄ yr⁻¹ under the RCP8.5. The magnitude of the growth is relatively small compared to Tan *et al* (2015a) and Tan and Zhuang (2015b) who predicted an 80% increase in Northern Europe even under the RCP2.6 scenario. It is likely because we did not model ebullition emission. It has been found that future warming may have much larger effects on ebullition even altering diffusive-emission dominant lakes to ebullition-dominant ones (Aben *et al* 2017). Therefore, the amount of extra increase is likely due to the enhanced ebullition processes.

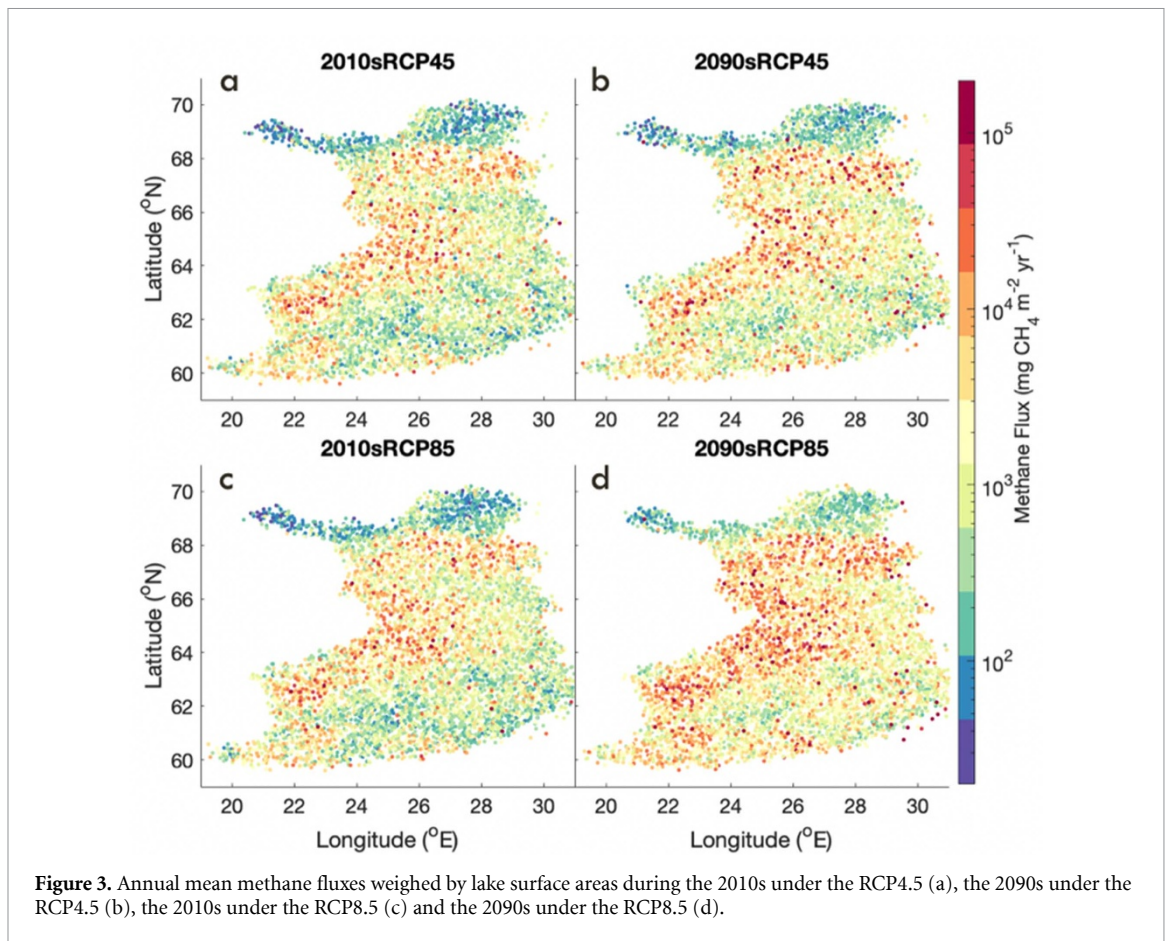
Based on the analysis of 297 lakes worldwide, Sanches *et al* (2019) found that considering only diffusive emissions would cause an average underestimation of 277%. By taking into account the ebullition emissions, the current annual methane emission for all northern lakes would be 13.76 ± 3.99 Tg CH₄ yr⁻¹, in the lower range of the previous estimation, 24.2 ± 10.5 Tg CH₄ yr⁻¹ by Walter *et al* (2007) and about the same as the 16.5 ± 9.2 Tg CH₄ yr⁻¹ by Wik *et al* (2016). Furthermore, Aben *et al* (2017)

predicted that ebullition would increase faster than diffusive emissions, by 51% with 4 °C warming. Similarly, Thornton *et al* (2015) predicted an increase of around 56% from the present to the 2040–2079 period using observations from three subarctic lakes in Sweden. If, based on the warming magnitude, we estimate a 50% and 100% growth of ebullition emissions under the RCP4.5 and RCP8.5, respectively, this will result in a total methane emission of 20.02 ± 5.8 Tg CH₄ yr⁻¹ and 27.97 ± 8.11 Tg CH₄ yr⁻¹, respectively from the whole Arctic lakes. This projection is slightly lower than the previously modelled 32.7 ± 5.2 Tg CH₄ yr⁻¹ from lakes north of 60 °N using the GLWD map by Tan *et al* (2015b). Their potential overestimation can result from: (1) They calibrated the model using only five lakes, four of which are thermokarst lakes that are found to have higher ebullition to diffusive emission ratio than other types of lakes (Wik *et al* 2016). According to their observation, this ratio can be over 30 which is much higher than we assumed; (2) They also assigned a shallow depth of 3 m to all lakes missing depth information, leading to even more overestimation of the ebullition emission (Joyce and Jewell 2003, Bastviken *et al* 2004, Del Sontro *et al* 2016).

3.3. Spatial variation in methane emissions and response to warming

Methane emissions are generally highest in regions dense with small lakes (figures 1(a) and 3), a pattern which was also found in previous studies (Bastviken *et al* 2004, Saarnio *et al* 2009, Del Sontro *et al* 2016, Wik *et al* 2016). This finding can be explained with two mechanisms. First, methane can be oxidized along diffusive transportation, and thus deeper lakes usually mean more loss by oxidation. Second, it was found that smaller lakes are more likely to have abundant organic substrates in their sediments, and thus they are potentially more productive for methane.

Interestingly, the southern and the northern part of Finland show different trends. By the same 4 °C of air temperature warming (figure S2), the south experiences a much more severe increase in emissions than the north (figure S3). Here we define the south and north be distinguished by latitude 67.5 °N, which north and south mean annual air temperature is above or below 0 °C in the 2010s, respectively. Therefore, the absolute increase in air temperature is not a complete proxy for emission. Instead, we found that the length of ice-free days plays a key role. By the end of the century, the mean ice-free days in the north are extended by 10.8% and 23.5% under RCP4.5 and RCP8.5, respectively while they are extended by 13.2% and 34.1%, respectively in the south (table S3). Methane fluxes can be blocked by ice cover and then oxidized in the water column during ice-on seasons. Therefore, a large amount of methane



trapped by ice cover currently could be emitted into the atmosphere in the future. Generally, ice covers of lakes in the north are thicker and thus would take more energy input to melt before methane can be released in winter.

The influence of ice-on days is further verified by the seasonality of emission (figure 4). From May to November, the warming climate affects emission in a similar pattern in both regions. However, the difference is shown in the south from December to April when we hardly see any emissions in the 2010s, but we expect much higher emissions in the future for the period due to warming. Such a shift may not be initiated in the north within this century and thus, the increase of emission in the north is much less severe. Wik *et al* (2014, 2016) also indicated that the ice-free days could potentially be the primary proxy for emission based on the observation of three lakes. Here, we confirm the finding with all the lakes in Finland and further verify it from a seasonality perspective. They predicted a 30% increase in total emission from northern lakes within the century by assuming a 20-day increase of ice-free days for all lakes. However, we emphasize that differentiating assumptions on ice-free day increase among regions is necessary for better precision in the estimation of regional budgets and future projections. Additionally, our simulated increase of ice-free days under RCP8.5 is two to three

times higher than their assumption, indicating an underestimation in the previous study.

3.4. Uncertainty quantification

Our model simulations did not consider the impacts of DOC dynamics on lake methane emissions. Boreal lakes, in addition to the climate change, have experienced moderate to severe browning over the last decades, probably due to the increased import of DOC from soils (Roulet *et al* 2006, Monteith *et al* 2007, Haaland *et al* 2010, Larsen *et al* 2011, Seekell *et al* 2015, Isidorova *et al* 2016). If DOC concentrations increase at the current rate, they can be doubled by the end of this century (de Wit *et al* 2016). It is found that methane diffusive methane emission is positively related to DOC concentrations (Sanches *et al* 2019). However, the relationship can involve several processes. More nutrients will be available for microbes and primary producers. However, the resulting increases in turbidity will weaken photosynthesis and thus oxygen production which limits methane oxidation. The model will need to be improved to predict the effect of lake browning. So far, no study has included this effect when estimating future emissions.

We assumed a constant landscape in our simulations that no lake expansion or drainage was considered until 2100. This is because boreal lakes

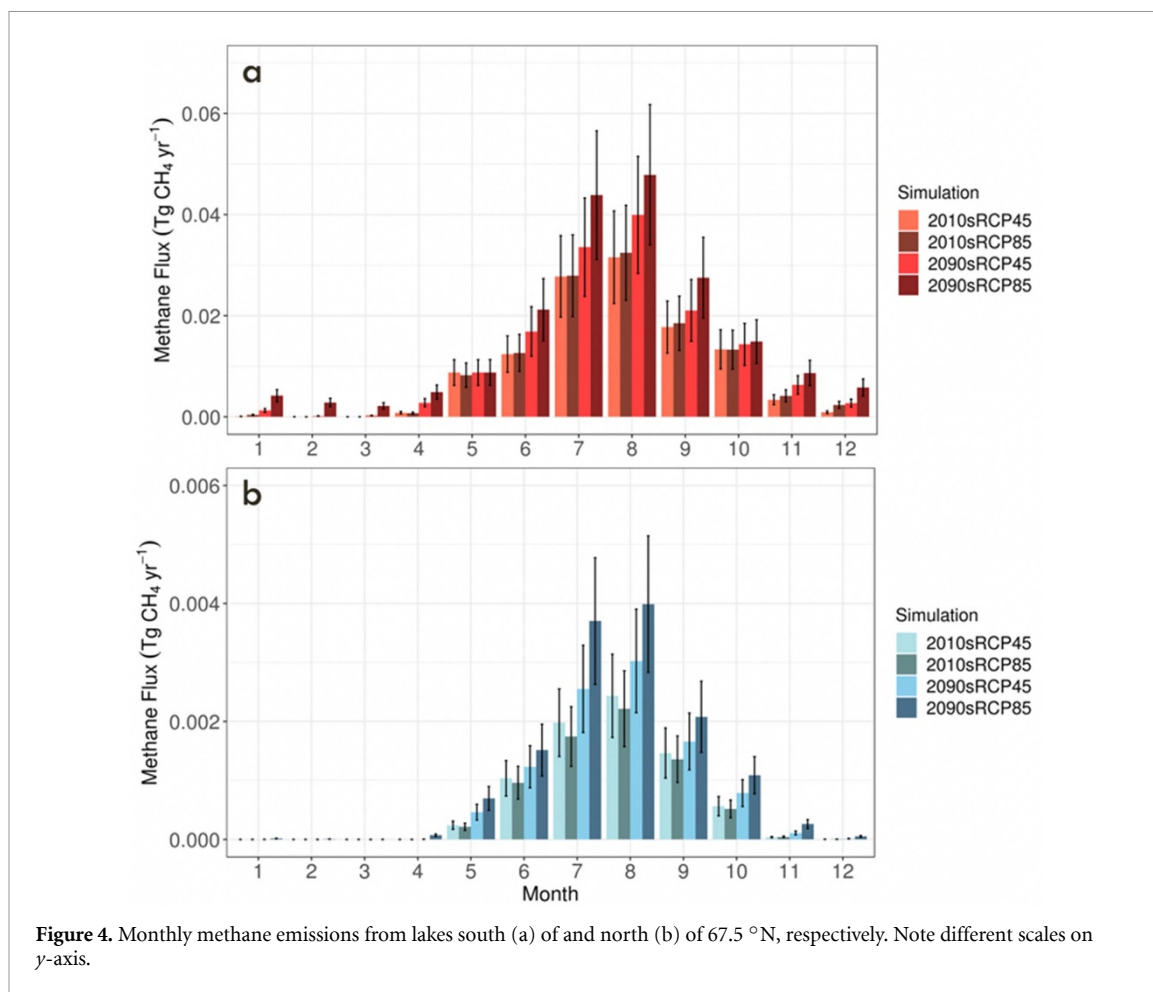


Figure 4. Monthly methane emissions from lakes south (a) of and north (b) of 67.5 °N, respectively. Note different scales on y-axis.

in Finland are not formed over permafrost and thus not affected by the active response of thawing and groundwater penetration processes in responding to climate as thermokarst lakes (van Huissteden *et al* 2011, Katey *et al* 2018). Wik *et al* (2016) predicted that with a 20-day increase of ice periods, even the total lake area decreases by 30%, the total methane emission can still grow by 20% which is 10% less than assuming constant lake area. Therefore, we will still expect the boreal lake methane emissions will be affected by considering the lake area changes. Incorporating lake areal dynamics into future quantification is necessary.

4. Conclusions

Lakes are an important component of the arctic and subarctic landscape. Our process-based lake biogeochemistry model simulation reveals that diffusive methane emissions from boreal lakes in Finland amount to 0.12 ± 0.03 Tg CH₄ yr⁻¹ during the 1990s and will increase by 25.8%–58.9% by the end of the 21st century depending on the warming scenario. There are two main driving factors. We find that higher air temperature will lead to higher lake water temperature and thus more active methanogenesis. Warming also results in shorter ice-on periods,

leading to longer emission days. The ice-free days are a more dominant factor than the lake temperature change impacts. If extrapolating the ratio of diffusion to ebullition emissions to the region, we estimated the annual regional lake emissions are 13.76 ± 3.99 Tg CH₄ yr⁻¹ at the present and 20.02 ± 5.8 – 27.97 ± 8.11 Tg CH₄ yr⁻¹ during 2090–2099 from all lakes north of 45 °N. Apart from climate forcing, lake trophic state, which we lack observation and future projection of, can also affect lake carbon and methane dynamics significantly. A more accurate estimation of lake methane emission requires both an increase in field measurement and improvement of the model structure. Furthermore, incorporating landscape evolution including lake drainage and expansion will refine our quantification of lake methane emissions in the future.

Acknowledgments and Data

This study is supported through a projected funded to Q Z by NASA (NNX17AK20G) and a project from the United States Geological Survey (G17AC00276). Z T is supported by the U.S. DOE's Earth System Modeling program through the Energy Exascale Earth System Model (E3SM) project. Narasinha Shurpali

acknowledges support from the CAPTURE project (Project No. 296887, Academy of Finland). The supercomputing is provided by the Rosen Center for Advanced Computing at Purdue University. The Ranta10 dataset is available at https://www.syke.fi/en-US/Open_information/Spatial_datasets/Downloadable_spatial_dataset#R. The model input and output data that support the findings of this study are openly available at <https://purr.purdue.edu/publications/3391/1>.

References

- Aben R C H, Barros N, Van Donk E, Frenken T, Hilt S Kazanjian G et al 2017 Cross continental increase in methane ebullition under climate change *Nat. Commun.* **8** 1682
- Bastviken D, Cole J, Pace M and Tranvik L 2004 Methane emissions from lakes: dependence of lake characteristics, two regional assessments, and a global estimate *Global Biogeochem. Cycles* **18** 4
- Bastviken D, Tranvik L J, Downing J A, Crill P M and Enrich-Prast A 2011 Freshwater methane emissions offset the continental carbon sink *Science* **331** 50–50
- de Wit H A, Valinia S, Weyhenmeyer G A, Futter M N, Kortelainen P, Austnes K et al 2016 Current browning of surface water will be further promoted by wetter climate *Environ. Sci. Technol. Lett.* **3** 430–5
- Dee D P, Uppala S M, Simmons A J, Berrisford P, Poli P, Kobayashi S and Bechtold P 2011 The ERA-Interim reanalysis: configuration and performance of the data assimilation system *Q. J. R. Meteorol. Soc.* **137** 553–97
- Del Sontro T, Boutet L, St-Pierre A, Del Giorgio P A and Prairie Y T 2016 Methane ebullition and diffusion from northern ponds and lakes regulated by the interaction between temperature and system productivity *Limnol. Oceanogr.* **61** S62–S77
- Finnish Environment Institute. (2016). Shoreline10 (ranta10) and river network http://paikkatieto.ymparisto.fi/arccgis/rest/services/SYKE/SYKE_Rantaviiva/MapServer
- Frieler K et al 2017 Assessing the impacts of 1.5°C global warming – simulation protocol of the Inter-Sectoral Impact Model Intercomparison Project (ISIMIP-2b) *Geosci. Model Dev.* **10** 4321–45
- Guseva S, Bleninger T, Jöhnk K et al 2020 Multimodel simulation of vertical gas transfer in a temperate lake *Hydrol. Earth Syst. Sci.* **24** 697–715
- Haaland S, Hongve D, Laudon H, Riise G and Vogt R D 2010 Quantifying the drivers of the increasing colored organic matter in boreal surface waters *Environ. Sci. Technol.* **44** 2975–80
- Holgerson M A and Raymond P A 2016 Large contribution to inland water CO₂ and CH₄ emissions from very small ponds *Nat. Geosci.* **9** 222–6
- Isidorova A, Bravo A G, Riise G, Bouchet S, Bjorn E and Sobek S 2016 The effect of lake browning and respiration mode on the burial and fate of carbon and mercury in the sediment of two boreal lakes *J. Geophys. Res.* **121** 233–45
- IPCC 2014 *Climate Change 2014: Synthesis Report. Contribution of Working Groups I, II and III to the Fifth Assessment Report of the Intergovernmental Panel on Climate Change* ed Core Writing Team, R K Pachauri and L A Meyer (Geneva: IPCC)
- Joyce J and Jewell P W 2003 Physical controls on methane ebullition from reservoirs and lakes *Environ. Eng. Geosci.* **9** 167–78
- Juutinen S, Rantakari M, Kortelainen P, Huttunen J T, Larmola T Alm J et al 2009 Methane dynamics in different boreal lake types *Biogeochemistry* **6** 209–23
- Katey W A, Thomas S V D, Ingmar N, Steve F, Abraham E Ronald D et al 2018 21st-century modeled permafrost carbon emissions accelerated by abrupt thaw beneath lakes *Nat. Commun.* **9** 3262
- Kirschke S, Bousquet P, Ciais P, Saunio M and Zeng G 2013 Three decades of global methane sources and sinks *Nat. Geosci.* **6** 813–23
- Kortelainen P, Mattsson T, Finér L, Ahtiainen M, Saukkonen S and Sallantausta T 2006 Controls on the export of C, N, P and Fe from undisturbed boreal catchments, Finland *Aquat. Sci.* **68** 453–68
- Larsen S, Andersen T and Hessen D O 2011 Climate change predicted to cause severe increase of organic carbon in lakes *Global Change Biol.* **17** 1186–92
- Lashof D A and Ahuja D R 1990 Relative contributions of greenhouse gas emissions to global warming *Nature* **344** 529–31
- Mattsson T, Kortelainen P and Räike A 2005 Export of DOM from boreal catchments: impacts of land use cover and climate *Biogeochemistry* **76** 373–94
- Mazumder A and Taylor W D 1994 Thermal structure of lakes varying in size and water clarity *Limnol. Oceanogr.* **39** 968–76
- Mcneall D J, Challenor P G, Gattiker J R and Stone E J 2013 The potential of an observational data set for calibration of a computationally expensive computer model *Geosci. Model Dev.* **6** 1715–28
- Monteith D, Stoddard J, Evans C et al 2007 Dissolved organic carbon trends resulting from changes in atmospheric deposition chemistry *Nature* **450** 537–40
- Mopper K and Qian J 2006 *Water Analysis: Organic Carbon Determinations. Encyclopedia of Analytical Chemistry Applications, Theory and Instrumentation* (New York: Wiley) (<https://doi.org/10.1002/9780470027318.a0884>)
- Myhre G et al 2013 Anthropogenic and Natural Radiative Forcing *In: Climate Change 2013: The Physical Science Basis. Contribution of Working Group I to the Fifth Assessment Report of the Intergovernmental Panel on Climate Change* T F Stocker, D Qin, G-K Plattner, M Tignor, S K Allen, J Boschung, A Nauels, Y Xia, V Bex and P M Midgley ed (Cambridge and New York: Cambridge University Press) pp 659–740
- Pighini S, Ventura M, Miglietta F and Wohlfahrt G 2018 Dissolved greenhouse gas concentrations in 40 lakes in the Alpine area *Aquat. Sci.* **80** 32
- Prairie Y and Del Giorgio P 2013 A new pathway of freshwater methane emissions and the putative importance of microbubbles *Inland Waters* **3** 311–20
- Raatikainen M and Kuusisto E 1990 The number and surface area of the lakes in Finland (in Finnish) *Terra* **102** 97–110
- Rachold V, Eicken H, Gordeev V V, Grigoriev M N, Hubberten H-W, Lisitzin A P et al 2014 Modern terrigenous organic carbon input to the Arctic Ocean *In the Organic Carbon Cycle in the Arctic Ocean* (Berlin: Springer) pp 33–55
- Roulet N and Moore T R 2006 Environmental chemistry: browning the waters *Nature* **444** 283–4
- Saarnio S, Winiwarer W and Leit O, J 2009 Methane release from wetlands and watercourses in Europe *Atmos. Environ.* **43** 1421–9
- Salter J M, Williamson D B, Scinocca J and Kharin V 2019 Uncertainty quantification for computer models with spatial output using calibration-optimal bases *J. Am. Stat. Assoc.* **1–24**
- Sanches L F, Guenet B, Marinho C C, Barros N and D. A. E. F 2019 Global regulation of methane emission from natural lakes *Sci. Rep.* **9**
- Sasaki M, Kim Y W, Uchida M and Utsumi M 2016 Diffusive summer methane flux from lakes to the atmosphere in the alaskan arctic zone *Polar Sci.* **S187396521630055X**
- Saunio M et al 2016 The global methane budget 2000–2012 *Earth Syst. Sci. Data* **8** 697–751
- Schilder J, Bastviken D, Van Hardenbroek M, Kankaala P, Rinta P, Stotter T et al 2013 Spatial heterogeneity and lake morphology affect diffusive greenhouse gas

- emission estimates of lakes *Geophys. Res. Lett.* **40** 5752–6
- Seekell D A, Lapierre J-F, Ask J, Bergstrom A-K, Deininger A, Rodriguez P and Karlsson J 2015 The influence of dissolved organic carbon on primary production in northern lakes *Limnol. Oceanogr.* **60** 1276–85
- Sobol' I M 1967 On the distribution of points in a cube and the approximate evaluation of integrals *USSR Comput. Math. Math. Phys.* **7** 86–112
- Tan Z, Yao H and Zhuang Q 2018 A small temperate lake in the 21st century: dynamics of water temperature, ice phenology, dissolved oxygen, and chlorophyll *a. Water Resour. Res.* **54** 4681–99
- Tan Z and Zhuang Q 2015b Methane emissions from pan-arctic lakes during the 21st century: an analysis with process-based models of lake evolution and biogeochemistry *J. Geophys. Res.* **120** 2641–53
- Tan Z, Zhuang Q, Shurpali N, Marushchak M, Biasi C, Eugster W and Walter Anthony K 2017 Modeling CO₂ emissions from Arctic lakes: model development and site-level study *J. Adv. Model. Earth Syst.* **9** 2190–213
- Tan Z, Zhuang Q and Walter Anthony K 2015a Modeling methane emissions from arctic lakes: model development and site-level study *J. Adv. Model. Earth Syst.* **7** 459–83
- Thornton B F, Wik M and Crill P M 2015 Climate-forced changes in available energy and methane bubbling from subarctic lakes *Geophys. Res. Lett.* **42** 1936–42
- van Huissteden J, Berrittella C, Parmentier F J W, Mi Y, Maximov T C and Dolman A J 2011 Methane emissions from permafrost thaw lakes limited by lake drainage *Nat. Clim. Change* **1** 119–23
- Walter K M, Smith L C and Stuart Chapin F 2007 Methane bubbling from northern lakes: present and future contributions to the global methane budget *Philos. Trans. R. Soc. London, Ser. A* **365** 1657–76
- Wik M, Thornton B F, Bastviken D, Macintyre S, Varner R K and Crill P M 2014 Energy input is primary controller of methane bubbling in subarctic lakes *Geophys. Res. Lett.* **41** 555–60
- Wik M, Varner R K, Anthony K W, Macintyre S and Bastviken D 2016 Climate-sensitive northern lakes and ponds are critical components of methane release *Nat. Geosci.* **9** 99–105
- Williamson D, Blaker A T, Hampton C and Salter J 2015 Identifying and removing structural biases in climate models with history matching *Clim. Dyn.* **45** 1299–324
- Williamson D, Blaker A T and Sinha B 2016 Tuning without over-tuning: parametric uncertainty quantification for the nemo ocean model *Geosci. Model Dev. Discuss.* 1–41
- Williamson D, Goldstein M, Allison L, Blaker A, Challenor P, Jackson L and Yamazaki K 2013 History matching for exploring and reducing climate model parameter space using observations and a large perturbed physics ensemble *Clim. Dyn.* **41** 1703–29
- Woolway R I, Jones I D, Maberly S C, French J R, Livingstone D M, Monteith D T et al 2016 Diel surface temperature range scales with lake size *PLoS ONE* **11** e0152466
- Woolway R I and Merchant C J 2017 Amplified surface temperature response of cold, deep lakes to inter-annual air temperature variability *Sci. Rep.* **7** 4130
- Yun Q, Jackson C, Giorgi F et al 2016 Uncertainty quantification in climate modeling and projection *Bull. Am. Meteorol. Soc.* **97** 821–4